EXCITATION TEST FOR EXPERIMENTAL MODELE OF SEMI-ACTIVE SEISMIC ISOLATION SYSTEM WITH CONTROLLABLE FRICTION DAMPER USING PIEZOELECTRIC ACTUATORS

Eiji SATO[1] and Takafumi FUJITA[2]

ABSTRACT: A semi-active seismic isolation system using a controllable friction damper was developed to decrease the relative displacement between the ground and a superstructure. Performance of the controllable friction damper is hampered, however, when the controller and the actuator malfunction during a large earthquake. In this study, a new controllable friction damper, using dependable piezoelectric actuators, is proposed as a solution. This damper has a fail-safe mechanism enabling the system to demonstrate a damping effect during malfunctions. This paper reports the results of excitation tests for a semi-active seismic isolation system using this controllable friction damper.

Key Words: *semi-active seismic isolation system, controllable friction damper, piezoelectric actuator*

INTRODUCTION

To decrease response acceleration of superstructures during an earthquake, several base-isolated buildings have been constructed using passive isolation systems (Fujita 1991a). The trade-off is that large relative displacement is inevitable in the passive seismic isolation system in order to decrease the response acceleration of the superstructures.

To solve this trade-off problem, a semi-active seismic isolation system using a controllable friction damper was developed in which the damping force was controlled by varying the pressure between the friction materials (Fujita 1991b, Fujita 1992). However, if the controller and the actuators, which press the friction material, malfunction, the damping force cannot be generated at all.

To solve this problem, a new controllable friction damper with a fail-safe mechanism was produced (Sato 2002, Sato 2003). To simplify the mechanism, dependable piezoelectric actuators, that are compact, can generate a large force and respond quick, are used. Simulations of the semi-active seismic isolation system with this controllable friction damper were performed to examine the seismic isolation and the relative displacement reduction. Several experiments were conducted to obtain characteristics of this controllable friction damper. A numerical model of the controllable friction damper was developed using the results of these experiments.

This paper reports the results of excitation tests for the semi-active seismic isolation system with this controllable friction damper to establish the semi-active isolation and the relative displacement reduction.

---

[1] Cooperative Research Fellow
[2] Professor

CONTROLLABLE FRICTION DAMPER

A controllable friction damper of the conventional system, (hereafter referred to as "holding type controllable friction damper"), generates friction force by pressing friction materials with actuators. Figure 1 illustrates the mechanism of the holding type controllable friction damper. The relationship between the actuator force and the friction force is expressed by

$$f(t) = \mu p(t) \tag{1}$$

where $f(t)$ is the friction force, μ is the friction coefficient, and $p(t)$ is the actuator force.

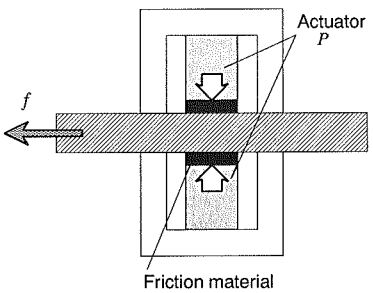

Figure 1 Holding type controllable friction damper

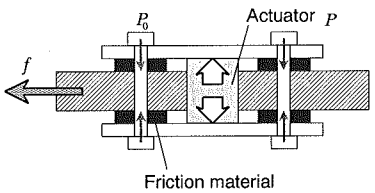

Figure 2 Releasing type controllable friction damper

When static, the actuator force is 0; therefore the friction force is 0. When an earthquake occurs, the damping force of the controllable friction damper is generated by controlling the actuator force. However, if a large earthquake occurs, the power source to the drivers of the controllable friction damper's controller and the actuators may be cut off. In such a case, this damper cannot generate the friction force, and the damping force is 0. The building acts as a low-damping isolation system then because the relative displacement is great and serious damage may occur by collision with surrounding structures.

To solve this problem, a controllable friction damper with a fail-safe mechanism is proposed. Damping force in the proposed damper, (hereafter referred to as "releasing type controllable friction damper"), can be generated in such a case. Figure 2 illustrates the mechanism of the releasing type controllable friction damper. The relationship between the actuator force and the friction force is expressed by

$$f(t) = \mu\left(p_0 - p(t)\right) \tag{2}$$

where $f(t)$ is the friction force, μ is the friction coefficient, p_0 is the initial pressure, and $p(t)$ is the actuator force.

In the initial state, the friction materials are pressed. Once an earthquake occurs, the actuator force is applied to reduce the friction by releasing the pressure between the friction materials. The friction force can be changed by controlling the actuator force. Even if the controller and the actuators of this damper malfunction and the actuator force $p(t)$ becomes zero, the damping force can be generated by the initial pressure p_0. Therefore, this system can prevent serious damage to the base-isolated structure by preventing collision with surrounding structures when the power supply fails or malfunctions occur.

RELEASING TYPE CONTROLLABLE FRICTION DAMPER

Mechanism

Figure 3 illustrates the drawing and sections of the releasing type controllable friction damper produced for experimental use. The initial pressure p_0 is generated by two pressure bolts, one each on top and bottom of the center.

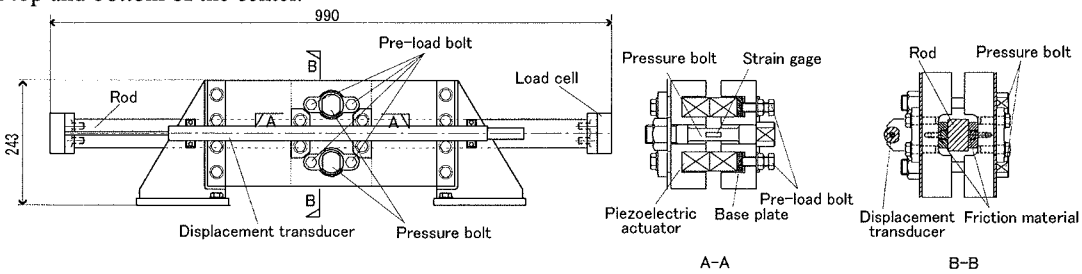

Figure 3 Drawing and sections of the releasing type controllable friction damper

In total, eight piezoelectric actuators are set up in four locations on both sides of these pressure bolts. Therefore, the releasing force is generated with the piezoelectric actuators. Figure 4 shows the piezoelectric actuator (Shimazaki 1996). The size is 25x25x36 mm, the maximum driving voltage is 100V, the range displacement is $20\text{x}10^{-6}$m, and the range generation force of the piezoelectric actuator is 20kN. Figure 5 demonstrates the relationship between the generation force and the displacement. Figure 6 demonstrates the relationship between the applied voltage and the displacement. The hysteresis in this relationship is not believed to be a problem in this research.

The pre-load of the piezoelectric actuators is adjusted with the pre-load bolts to adjust the generation force and displacement of the piezoelectric actuator.

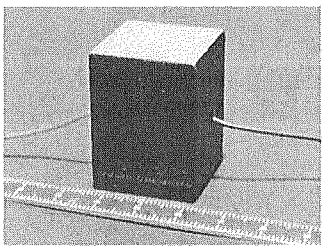

Figure 4 Piezoelectric actuator

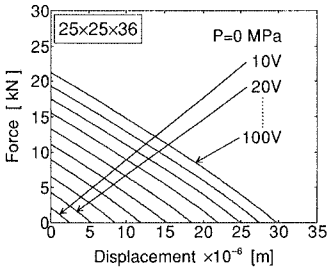

Figure 5 Relationship of generation force and displacement

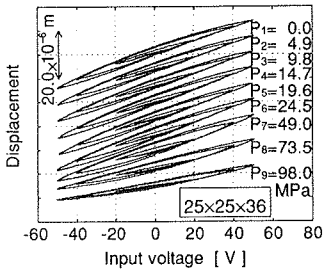

Figure 6 Relationship of applied voltage and displacement

Characterization

Figure 7 and Figure 8 demonstrate the friction force of the damper at four different sliding velocities, when 0 V and 100V were applied to the piezoelectric actuators, respectively. These figures indicate that the friction force is constant, independent of the sliding velocity.

Figure 9 illustrates the relationship between the voltage applied to the piezoelectric actuators and the friction force of the damper when the sinusoidal voltage applied to the piezoelectric actuators was changed from 0V to 100V. Hysteresis and nonlinearity exist in the relationship between the applied voltage and the friction force. This hysteresis is related to the hysteresis of the piezoelectric actuators. The nonlinearity is an influence of the saturation of the minimum friction force. However, this relationship is approximated as a linear function for simplification. The approximated linear function is

$$f = 2.97 - 0.0312E \tag{3}$$

where f [kN] is the friction force of the controllable friction damper of releasing type and E [V] is the voltage applied to the piezoelectric actuators.

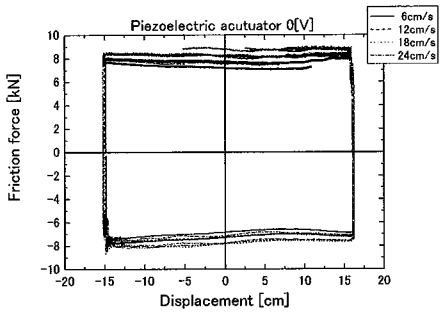

Figure 7 Result of velocity dependence test (0 V applied)

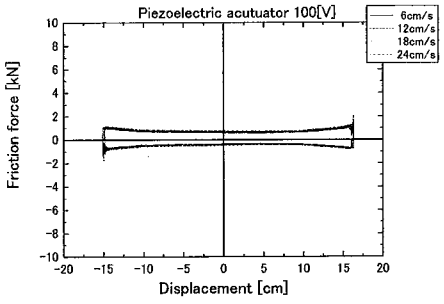

Figure 8 Result of velocity dependence test (100 V applied)

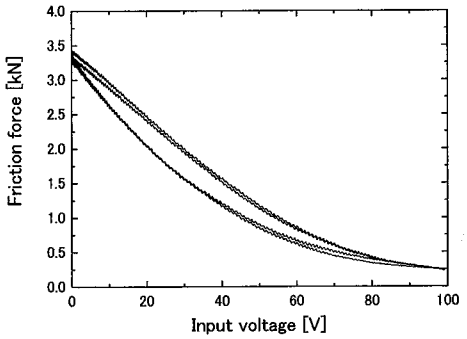

Figure 9 Applied voltage and friction force relationship

SHAKE TABLE TEST FOR SEMI-ACTIVE SEISMIC ISOLATION SYSTEM

Base-isolation building model

The building model used for the tests consists of a steel skeleton frame and steel plate weights, and is supported by four linear bearings. Figure 10 shows the test building model. The superstructure and base frame are connected with coil springs and the releasing type controllable friction damper. The total mass of the superstructure is 6350 kg. The first mode natural frequency of the isolation system is 0.33 Hz.

Control system

The control system consists of sensors, DSP, A/D-D/A converters, and a piezoelectric driver. The control voltage calculated by DSP is input into the piezoelectric driver. Figure 11 illustrates the control system.

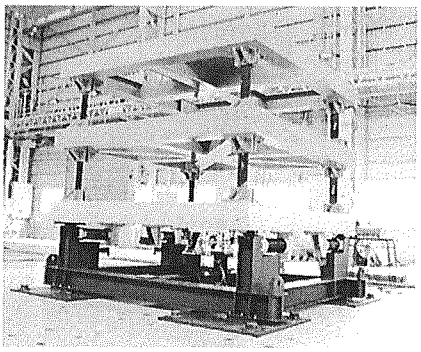

Figure 10 Test building model

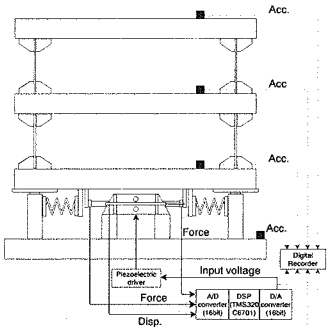

Figure 11 Control system

Analysis model

Figure 12 demonstrates that the seismic isolation system using the controllable friction damper is modeled as a three-degree-of-freedom system. Equations of motion of the model are expressed in two phases, as shown below, considering transition of static/dynamic friction due to the presence or absence of sliding at the friction damper.

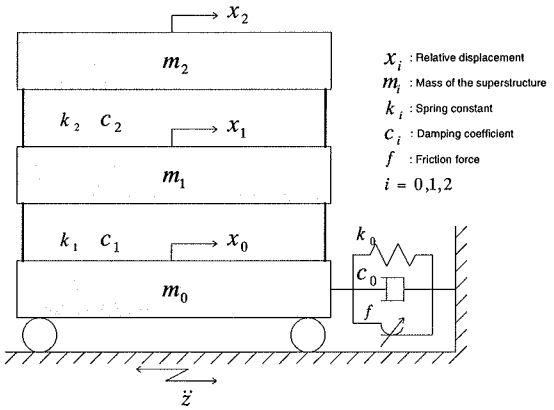

Figure 12 Analysis model

(1) Phase I No sliding at friction damper

$$\begin{cases} \dot{x}_0 = 0 \quad x_0 = const. \\ m_1\ddot{x}_1 + (c_1 + c_2)\dot{x}_1 - c_2\dot{x}_2 - k_1x_0 + (k_1 + k_2)x_1 - k_2x_2 = -m_1\ddot{z} \\ m_2\ddot{x}_2 - c_2\dot{x}_1 + c_2\dot{x}_2 - k_2x_1 + k_2x_2 = -m_2\ddot{z} \end{cases} \tag{4}$$

(2) Phase II Sliding at friction damper

$$\begin{cases} m_0\ddot{x}_0 + (c_0 + c_1)\dot{x}_0 - c_1\dot{x}_1 + (k_0 + k_1)x_0 - k_1x_1 + \mathrm{sgn}(\dot{x}_0)\mu(p_0 - p) = -m_0\ddot{z} \\ m_1\ddot{x}_1 - c_1\dot{x}_0 + (c_1 + c_2)\dot{x}_1 - c_2\dot{x}_2 - k_1x_0 + (k_1 + k_2)x_1 - k_2x_2 = -m_1\ddot{z} \\ m_2\ddot{x}_2 - c_2\dot{x}_1 + c_2\dot{x}_2 - k_2x_1 + k_2x_2 = -m_2\ddot{z} \end{cases} \tag{5}$$

The transition criteria between Phase I and Phase II are:

1) From Phase I to Phase II

$$|m_0\ddot{z} - c_1\dot{x}_1 + (k_0 + k_1)x_0 - k_1x_1| > \mu(p_0 - p) \tag{6}$$

2) From Phase II to Phase I

$$\begin{cases} \dot{x}_0 = 0 \\ |m_0\ddot{x}_0| < 2\mu(p_0 - p) \end{cases} \tag{7}$$

Linear quadratic optimum regulator theory

The optimal generation force is obtained by using linear quadratic optimum regulator theory (LQ). A performance index J is defined as follows (assuming that $u = f$):

$$J = \int_0^\infty \left\{\alpha(\ddot{x} + \ddot{z})^2 + \beta x^2 + \gamma u^2\right\} dt \tag{8}$$

where α, β, and γ are weighting coefficients.

The Linear Quadratic optimal regulator problem is solved, and the optimal control force of u^* is obtained. When semi-active control by the damping force of the controllable friction damper is considered, the direction of force generated by the damper depends on the conditions below.

$$u = \begin{cases} u^* & (u^* \cdot \dot{x} > 0) \\ 0 & (u^* \cdot \dot{x} < 0) \end{cases} \tag{9}$$

Instantaneous optimal control

When the releasing type controllable friction damper is used, the equation of motion of the seismic isolation system is nonlinear. An Instantaneous Optimal Control algorithm (IOC), which is effective on a nonlinear system, is used to obtain the optimal piezoelectric actuator force $p(t)$. Performance index $J(t)$ of IOC is defined as follows:

$$J = q_v\dot{x}^2(t) + q_dx^2(t) + q_fF^2(t) + E^2(t) \tag{10}$$

where $q_v \geq 0$, $q_d \geq 0$, and $q_f \geq 0$ are weighting coefficients.

The optimal piezoelectric actuator force $E^*(t)$ to minimize the performance function $J(t)$ is obtained as follows:

$$E^*(t) = -\frac{q_f a_f b_f}{m^2\left(1 + q_f\dfrac{a_f^2}{m^2}\right)} + \frac{q_v a_f \Delta t \operatorname{sgn}(\dot{x}(t))}{2m\left(1 + q_f\dfrac{a_f^2}{m^2}\right)\left(1 + \dfrac{\Delta t^2}{6}\omega^2 + \Delta t\zeta\omega\right)}\dot{x}(t)$$
$$+ \frac{q_d m a_f \Delta t^2 \operatorname{sgn}(\dot{x}(t))}{2m\left(1 + q_f\dfrac{a_f^2}{m^2}\right)\left(1 + \dfrac{\Delta t^2}{6}\omega^2 + \Delta t\zeta\omega\right)}x(t) \tag{11}$$

where μ is the friction coefficient and Δt is the sampling time.

Test result

Figure 13 illustrates the relative displacement and the response acceleration for the EL Centro NS (1940, Imperial Valley Earthquake) inputs when semi-active isolation controller is designed by LQ. The weighting coefficients of the performance index are selected so that acceleration can be smaller in LQ-1 and relative displacement can be smaller in LQ-2. 'P-1' and 'P-2' in the figures indicate passive seismic isolation using a friction damper with a constant pressure. In case P-1 (P-2), the pressure is set to begin to slide the friction damper if the input acceleration exceeds 10cm/s^2 (25cm/s^2).

Comparing LQ-1 with P-1, the response acceleration is almost the same, but the relative displacement of LQ-1 is decreased to about 60%. Additionally, comparing LQ-2 with P-2, the relative displacement is almost the same, but the response acceleration of LQ-2 decreased to about 60%. The expected effects are thus achieved in both LQ cases.

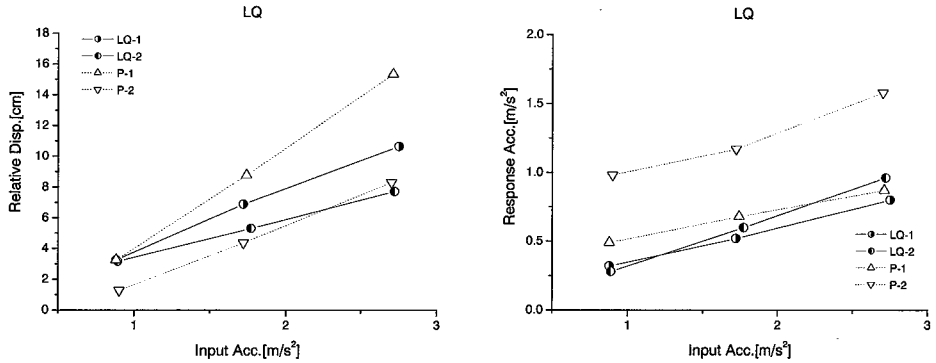

Figure 13 Relative displacement and response acceleration of LQ

Figure 14 shows the result of the IOC test. The weighting coefficients of the performance index are selected so that acceleration can be smaller in IOC-1 and relative displacement can be smaller in IOC-2. These figures also show the results of the passive seismic isolation.

Compared to P-1, the relative displacement of IOC-1 decreases to about 76% and 47% in IOC-2. The response acceleration of IOC-2 and P-1 is almost the same. However, the response acceleration of IOC-1 is smaller than that of IOC-2 and P-1. Compared to P-2, the response acceleration of IOC-1 decreases to about 50%, and to 55% in IOC-2. The expected effects are achieved in IOC as well as LQ.

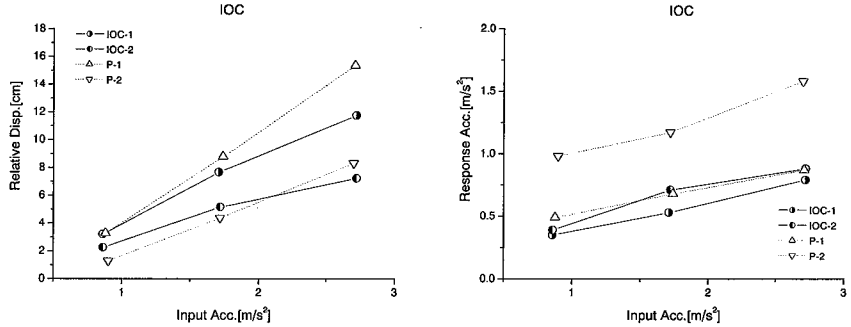

Figure 14 Relative displacement and response acceleration of IOC

Figure 15 illustrates the time-histories in LQ-1, IOC-1 and P-1. The input is EL Centro NS of 300cm/s^2. These figures also show the simulation results. The simulation results agree with experiment results as well, confirming that the analysis model is valid.

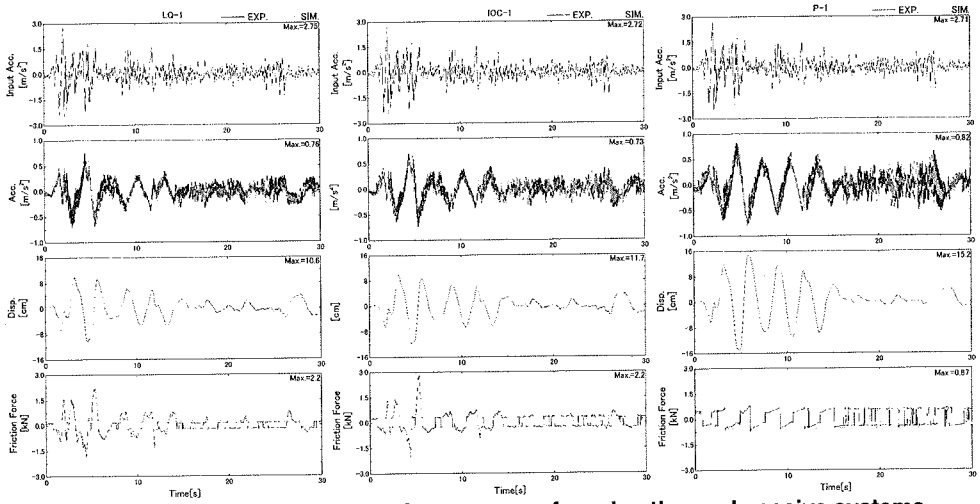

Figure 15 Time histories of responses of semi-active and passive systems (Experimental and simulation results)

CONCLUSIONS

A new controllable friction damper with a fail-safe mechanism was produced, and it was experimentally confirmed that the friction force of the releasing type controllable friction damper can be changed by controlling the piezoelectric actuator force.

The shaking table tests for a semi-active isolation system with this damper were conducted. The tests confirmed that the semi-active seismic isolation system with this controllable friction damper whose controller was designed LQ and IOC performs better than the passive seismic isolation system. The expected effects were achieved by selecting the weighting coefficient in each control rule of LQ and IOC.

References

Fujita, T. (1991a) "Research, development and application of seismic isolation systems in Japan, Proceeding of the International Meeting on Earthquake Protection of Builgings" Ancona, Italy,6-8, June, 77/C-90/C.

Fujita, T., Kabeya, K., Hayamizu, Y., Aizawa, S., Higashino, M., Kubo, T., Haniuda, N., and Mori, T., (1991b). "Semi-active seismic isolation system using controllable friction damper (1st report, Development of controllable friction damper and fundamental study of semi-active control system)" Trans. of Japan Soc. Mech. Eng. , 57, 536 Ser.C, 1122-1128 (in Japanese).

Fujita, T., Shimazaki, M., Hayamizu, Y., Aizawa, S., Higashino, M., Kubo, T., and Haniuda, N. (1992) "Semi-active seismic isolation system using controllable friction damper (2nd report, Study of the system with distributed controllable friction dampers)" Trans. of Japan Soc. Mech. Eng. , 58, 551 Ser.C, 2012-2016 (in Japanese).

Sato, E., Fujita, T., (2002) "Fundamental Analysis for Semi-active Seismic Isolation System with Controllable Friction Damper Using Piezoelectric Actuators" Bull. ERS, No. 35, 21-30.

Sato, E., Fujita, T., (2003) "Experiments of Controllable Friction damper Using Piezoelectric Actuators for Semi-Active Seismic Isolation System" Bull. ERS, No. 36, 57-70.

Shimazaki, M., and Fujita, T. (1996) "Experimental Study of Piezoelectric Actuator for Large-Scale Smart Structure (2nd Report, Actuator Characteristics of 25x25x36 Piezoelectric Actuator of Stack Type)" SEISAN-KENKYU Vol. 48, No. 9, 449-452 (in Japanese)